

Objective visual performance evaluation with visual evoked potential measurements based on an adaptive optics system

Yanrong Yang (杨彦荣)^{1,2,3}, Junlei Zhao (赵军磊)^{1,2}, Haoxin Zhao (赵豪欣)^{1,2},
Fei Xiao (肖飞)^{1,2}, Jiaxin Xie (谢佳欣)⁴, Tiejun Liu (刘铁军)⁴, and Yun Dai (戴云)^{1,2,*}

¹Key Laboratory on Adaptive Optics, Chinese Academy of Sciences, Chengdu 610209, China

²Laboratory on Adaptive Optics, Institute of Optics and Electronics, Chinese Academy of Sciences, Chengdu 610209, China

³University of Chinese Academy of Sciences, Beijing 100049, China

⁴School of Life Science and Technology, University of Electronic Science and Technology of China, Chengdu 610054, China

*Corresponding author: daiyun@ioe.ac.cn

Received January 23, 2018; accepted March 7, 2018; posted online April 24, 2018

An objective visual performance evaluation with visual evoked potential (VEP) measurements was first integrated into an adaptive optics (AO) system. The optical and neural limits to vision can be bypassed through this system. Visual performance can be measured electrophysiologically with VEP, which reflects the objective function from the retina to the primary visual cortex. The VEP measurements without and with AO correction were preliminarily carried out using this system, demonstrating the great potential of this system in the objective visual performance evaluation. The new system will provide the necessary technique and equipment support for the further study of human visual function.

OCIS codes: 330.4460, 220.1080, 330.4300, 330.1070, 330.1800.

doi: 10.3788/COL201816.053301.

Visual performance tests [visual acuity (VA) and contrast sensitivity (CS), etc.] provide important supplementary data for diagnosing visual pathology or other pathological involvement of the visual pathway. However, it is well known that visual performance is governed by optical, retinal, and neural factors. At present, several successful attempts have been directed at bypassing the optical limits. For example, the history can be traced back to when Campbell and Green^[1] measured the contrast sensitivity function (CSF) without optical limits using interference fringes formed on the retina. Aside from interference fringes, a powerful tool to bypass the optical limits was through adaptive optics (AO). Since Liang *et al.*^[2] first used the AO technique to obtain supernormal vision through high-order aberration (HOA) correction in 1997, a great deal of attention has been paid to the relationship between ocular aberrations and visual performance through the AO system. In 2011, Roorda^[3] made a more comprehensive review of the application of AO in vision.

However, all of the studies mentioned above were the optical limits to subjective visual performance. The subjective test is measured by the psychophysiological method. It always needs subjects to judge by a perceived pattern stimulus. Unfortunately, the subjective visual performance benefits obtained through AO correction were confounded with neural limits. Artal *et al.*^[4] have found that through AO the eye somehow adapted to the blur generated by its own point spread function (PSF) to

manipulate their aberrations in such a way to rotate the eye's native PSF. It meant that adaptation to our own aberrations limited the effectiveness of an aberration correction and was defined as neural insensitivity. In 2007, Chen *et al.*^[5] also showed that the sharpest image was generated with some remaining aberration rather than a full AO correction. It can be seen that the neural limits confounded the accurate assessment of visual performance with subjective tests.

Aside from subjective tests, visual performance can be measured by objective tests, which only need subjects to keep fixated on the stimuli, using the electrophysiological techniques of visual evoked potential (VEP)^[6], electroretinogram (ERG), and electrooculogram (EOG). Obviously, the objective tests have some advantages over subjective tests especially for infants, mental retardation, mental disorders, malingering, etc. Among these objective tests, VEP that represents the response of the visual vortex to visual stimuli has been shown to be valuable in assessing VA^[7] and CS^[8] objectively, especially in infants and individuals with short attention spans. In addition, the VEP is a useful tool to help with diagnosing visual pathway pathology objectively and is widely used in forensic practice.

But, as in the subjective tests, in order to measure retinal or visual pathway limits to vision by the objective VEP and other electrophysiological techniques, the optical limits should be first bypassed. As far as we know, using AO to bypass the optical limits in VEP measurement is a new technique. It has been found that using the VEP

measurements in visual performance tests appears to improve diagnostic power^[9,10]. It prompts us to consider the new technique of integrating VEP measurements into an AO system.

In this Letter, we report a setup of an objective visual performance evaluation system with VEP based on the AO system. The system will provide a platform for accurate assessment of visual performance with VEP measurements. Obviously, the new technique adds a new and reliable dimension to study the development of vision.

The preliminary research on VEP measurements without and with AO correction has been carried out on this system. Figure 1 is the schematic of the AO system integrated with pattern reversal VEP (PR-VEP) measurements. This system can be divided into an AO aberration manipulation subsystem and a PR-VEP measurement subsystem.

The AO aberration manipulation subsystem is mainly comprised of a wavefront sensor, a deformable mirror, and a closed-loop control system. The AO system design and layout analysis can be found elsewhere^[11,12]. We only introduce the part of optical path. A beacon superluminescent diode (SLD) (shown in Fig. 1) was collimated as a parallel light beam after it passed through a collimation lens L11 and spatial filter P, and then it passed and was reflected through the relevant optical channels to be directed into the subject's eye. The beacon light was focused on the subject's retina and the backward-scattered light exited through the pupil, passed through the deformable mirror, pupil matching, and relay optical system (L3-L4, L5-L6), and was then projected onto a Shack-Hartmann wavefront sensor (SHWS) to measure the wavefront slope G . G was processed by a computer, transformed into a voltage matrix V , and constructed into a wavefront matrix A by

$$V = C_{xy} G, \quad (1)$$

$$A = R_{xy} G, \quad (2)$$

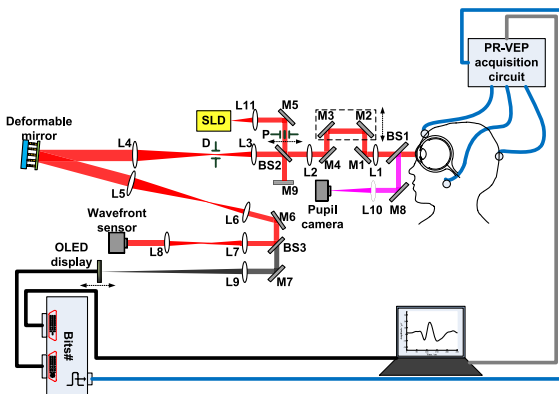


Fig. 1. AO system integrated with pattern reversal VEP (PR-VEP) measurements. SLD, superluminescent diode; BS, beam splitter; M, mirror; L, lens; P, artificial entrance pupil; D, diaphragm.

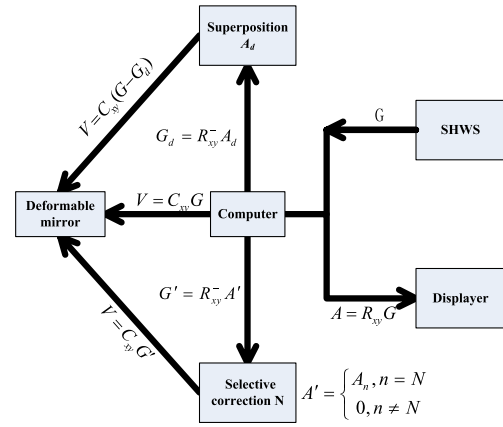


Fig. 2. Wavefront aberrations sensing and aberrations manipulation. R_{xy}^- , the pseudo inverse version of the reconstruction matrix; A' , selectively correcting the N th orders of Zernike aberrations; A_d , the Zernike coefficient values of superposition aberrations; G' , the wavefront slope matrix corresponding to A' ; G_d , the wavefront slope matrix corresponding to A_d .

where C_{xy} is a control matrix of an AO system and R_{xy} is a reconstruction matrix of SHWS, respectively. Figure 2 shows the process of aberration manipulation. The detailed analysis of aberration manipulation can be found in Ref. [13].

In the objective VEP measurements, the pattern stimuli can be presented in a pattern reversal way^[14]. After pattern reversal stimulation, the electrophysiological activities can be recorded from electrodes attached to the scale in the visual cortex. The activities were amplified by the VEP acquisition circuit^[15] (shown in Fig. 1). The bandpass of the amplifier was 1–30 Hz, and the digitization frequency was 1000 Hz. The recording computer was connected to the VEP acquisition circuit via a standard COM port. A single recording session yielded three VEPs in response to three repeated stimulations of 100 pattern reversal presentations in one type of stimulus. The resulting signals of PR-VEP were separated from the noise (electroencephalogram, EEG) by a filtering and averaging process using a customized MATLAB program.

The stimuli were displayed by an organic light-emitting diode (OLED, EMA-100100, eMagin Corporation) monochrome black-and-white microdisplay with an effective size of 12 mm × 8 mm, a resolution of 800 × 600 in pixels, and a highest refreshment rate of 75 Hz. According to the test conditions requirements, the luminance of the microdisplay could be manually adjusted. In order to produce gray levels with 14 bits of resolution, the stimulus pattern was input into the Bits# stimulus processor (Cambridge Research System), which transferred the pattern stimulus to the OLED display. The Bits# simultaneously sent a synchronizing signal to the PR-VEP measurement subsystem, including the accurate timing of the stimulus presentation. The synchronizing signal was delivered at every reversal in the stimulus. This was used to tag 100 responses and average to each type of stimulus. The trial

was restarted once the results of the 3 repeated measurements were not reproducible, and it was stopped after the second was not reproducible.

PR-VEP measurements were made in a dark room. The effective distance from the OLED's screen to the eye was 200 mm. The filled size on the screen was 2° . For the VA or CS tests, the stimulus was a vertical sinusoidal grating with different frequencies. The subjects were instructed to look at a cross in the center of the screen.

To monitor the fixation status of a subject in real time, the system was miniaturized and mounted in a three-axis motorized translation platform, as shown in Fig. 3. The pupil camera and the adjustment of the motorized translation stage would ensure that subjects' fixation was focused on the small cross in the center of the screen.

Based on the developed AO system integrated with PR-VEP measurements, three volunteers (DP, ZZ, and CKY) were used to PR-VEP measurements without and with AO correction. The detailed information for all subjects is shown in Table 1. The subject's low-order aberrations were always corrected by inserting the trial lens at the front of eye. Prior to the experiment, all participants signed an informed consent form. In the experiment, each subject was treated with dilation of pupils and paralysis of accommodation by administering 1% cyclopentolate.

During the PR-VEP measurements, a vertical sinusoidal grating with a contrast of 0.9 and different spatial frequencies of 4, 8, and 16 cycles per degree (cpd) were used as the pattern stimulus. The reversal stimulation time frequency was 2 Hz or 4 reversals per second (rps).

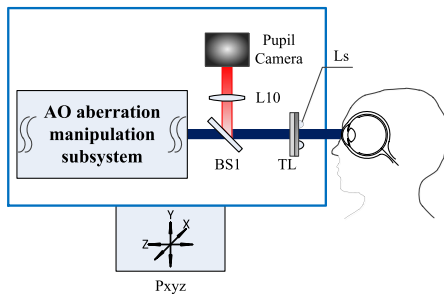


Fig. 3. Schematic of the miniaturized AO system. L, lens; BS, beam splitter; TL, trial lens holder; Ls, LED source; Pxyz, three-dimensional traveling platform.

Table 1. Detailed Information for All Subjects

| Subject | Refractive error | | Age | Sex |
|---------|------------------------------------|-----------------------------------|----------|-----|
| | OD | OS | | |
| DP | -0.75 | -2.00 - 0.25 $\times 15^\circ$ | 22 years | F |
| ZZ | -1.25 | -0.75 | 24 years | M |
| CKY | -1.50 - 0.25 $\times 150^\circ$ | 0.25 - 0.25 $\times 19^\circ$ | 20 years | M |

The PR-VEP waveforms at each spatial frequency were recorded without and with AO correction.

Figure 4 shows the measured Zernike coefficient values and the corresponding PSF (calculated by numerical method) for one typical subject CKY under the two correction strategies. The aberrated PSF distorts and reduces the contrast of the stimulus and, as a result, blurs an image primarily with high spatial frequencies. After AO correction, all the aberrations up to seven-order radial Zernike modes were corrected, and the residual RMS aberrations converged to a small value of about $0.1 \mu\text{m}$, demonstrating a good performance of the AO system. Also, the aberrated PSF became compact and approached near diffraction-limited.

Figure 5 compares the PR-VEP waveforms of three subjects under the two correction strategies. After AO correction, it not only improved the subjective VA and CS^[13], but also increased the negative-position-negative (NPN) amplitudes of the waveform with varying degrees. The results were consistent with PSF changes with AO correction.

For further analysis, the eigenvalues of NPN waveforms in the PR-VEP were extracted; that is, the first negative wave N1, the first positive wave P1, and the second negative wave N2, including amplitudes and latencies. The amplitude of N1 is absolute, the amplitudes of P1 and N2 are P1-N1 and P1-N2, respectively; the latency of N1, P1, and N2 is the time from the stimuli presentation to the appearance of positive or negative waves.

Figure 6 is the average NPN amplitudes and latencies of all eyes from three subjects. The black histogram shows the magnitude and latency with AO correction. Compared with no AO correction (red histogram), after AO correction the amplitudes of NPN at all spatial frequencies were increased with statistical significance ($p < 0.05$). The increased amplitude meant that the subject received a clearer stimulus and the decreased amplitude meant that

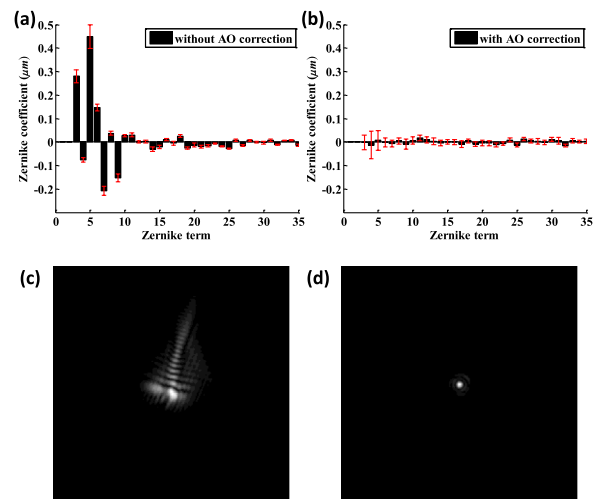


Fig. 4. (a), (b) Zernike coefficient values, and (c), (d) PSF of subject CKY without and with AO correction. (a), (c) without AO correction. (b), (d) with AO correction.

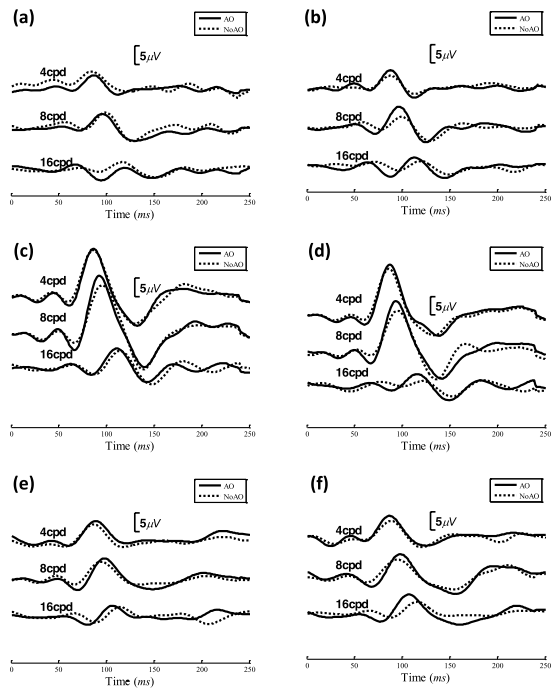


Fig. 5. PR-VEP waveform comparison of three subjects without and with AO correction. (a) and (b) are the right and left eye of DP, respectively. (c), (d) and (e), (f) correspond to ZZ and CKY, respectively.

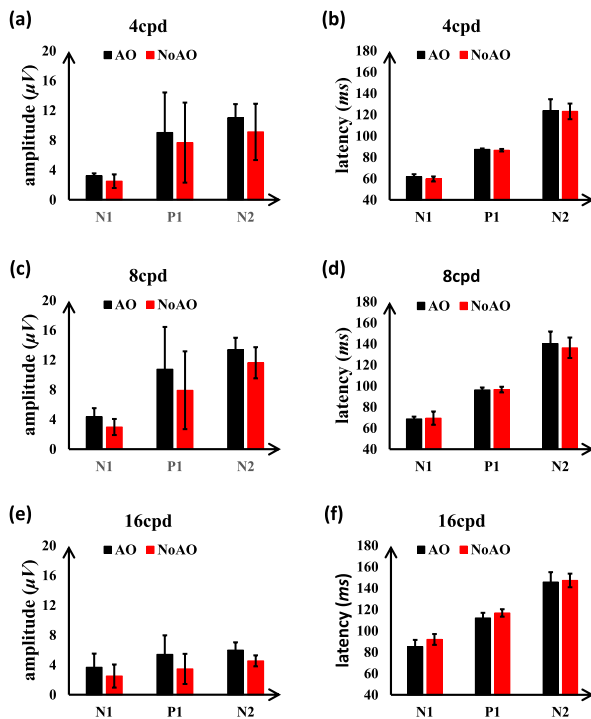


Fig. 6. Average NPN magnitude and latency of all eyes from three subjects. The first column (a), (c), (e) are the amplitudes at 4, 8, 16 cpd, respectively. The second column (b), (d), (f) are the latencies at 4, 8, 16 cpd, respectively.

the subject received a blurred stimulus. As a result, the amplitude of NPN was equivalent to the subjective perception. According to this equivalent principle,

PR-VEP can be used to objectively measure refractive power^[16] and to objectively evaluate VA and CSF^[7-9]. However, the change of latency in each spatial frequency was not obvious, and it had no statistical significance.

These differences of NPN amplitudes and latencies after AO corrections could be interpreted that it improved retinal image quality and not changed the spatial frequencies and field size. While NPN amplitude reflected the number of excited nerve fibers that reached the visual cortex, NPN latency reflected the different transmission channel. As a result, more nerve cells were excited with AO corrections, and then the NPN amplitude was increased.

In conclusion, we integrated an objective visual performance evaluation with PR-VEP measurements into the AO system. It first used AO aberration manipulation technology in the PR-VEP measurements. The performance of the system was checked with objective PR-VEP measurements experiments without and with AO corrections. The results showed that the PR-VEP measurement was an objective and quantitative tool for studying the relationship between the ocular aberrations and visual performance that reflected the retinal and visual pathway limits to vision. Bypassing the optical and neural limits to vision, the PR-VEP measurements based on AO would be an accurate visual performance evaluation.

In addition, the subjective visual performance (VA and CS) tests and objective PR-VEP measurements can be taken under the same system. It was convenient and possible to compare between the two metrical methods. Also, the two metrics can be used to confirm each other. In these respects, the system provided the necessary technical and equipment support for future research on visual function.

The future work will be focused on using this system to study whether the subjective or objective evaluating method has the same sensitivity for visual performance changes and whether they reflect the same aspects of visual performance. Then, it is valuable to find subclinical markers of visual performance decline. Besides, this technique can be transited to binocular vision to assess binocular visual function with both subjective and objective metrical methods and in depth to understand the mechanism of binocular vision formation and binocular visual function maintenance.

The authors would like to thank all the subjects for their positive supports in this work. This research was supported by the National Natural Science Foundation of China (No. 61378064) and the National High Technology Research and Development Program of China (No. 2015AA020510).

References

1. F. W. Campbell and D. G. Green, *J. Physiol.* **181**, 576 (1965).
2. J. Liang, D. R. Williams, and D. T. Miller, *J. Opt. Soc. Am. A* **14**, 2884 (1997).
3. A. Roorda, *J. Vision* **11**, 6 (2011).
4. P. Artal, L. Chen, E. J. Fernandez, B. Singer, S. Manzanera, and D. R. Williams, *J. Vision* **4**, 281 (2004).

5. L. Chen, P. Artal, D. Gutierrez, and D. R. Williams, *J. Vision* **7**, 9 (2007).
6. K. Xiong, M. Hou, and G. Ye, *Chin. Opt. Lett.* **3**, 432 (2005).
7. K. K. Iyer, A. P. Bradley, and S. J. Wilson, *Doc. Ophthalmol.* **126**, 21 (2013).
8. A. M. Norcia, C. W. Tyler, R. D. Hamer, and W. Wesemann, *Vis. Res.* **29**, 627 (1989).
9. S. N. Abdullah, G. F. Sanderson, A. C. James, and T. M. Vaegan, *Doc. Ophthalmol.* **128**, 111 (2008).
10. I. Sun, J. Lee, H. Huang, and H. Kuo, *Doc. Ophthalmol.* **130**, 221 (2015).
11. Y. Wang, Y. He, L. Wei, X. Li, J. Yang, H. Zhou, and Y. Zhang, *Chin. Opt. Lett.* **15**, 121102 (2017).
12. Z. Wang, G. Shi, and Y. Zhang, *Chin. Opt. Lett.* **12**, S11103 (2014).
13. Y. Dai, L. Zhao, F. Xiao, H. Zhao, H. Bao, H. Zhou, Y. Zhou, and Y. Zhang, *Appl. Opt.* **54**, 979 (2015).
14. F. Almoqbel, S. J. Leat, and E. Irving, *Ophthalmic Physiol. Opt.* **28**, 393 (2008).
15. D. Gao, T. Liu, J. Cai, X. Shi, C. Ding, P. Xu, and D. Yao, *IFMBE Proc.* **39**, 1483 (2013).
16. D. Regan, *Invest. Ophthalmol.* **12**, 669 (1973).